

**UNCLASSIFIED**

---

**AD**

**402 337**

*Reproduced  
by the*

**DEFENSE DOCUMENTATION CENTER**

FOR

**SCIENTIFIC AND TECHNICAL INFORMATION**

CAMERON STATION, ALEXANDRIA, VIRGINIA



---

**UNCLASSIFIED**

NOTICE: When government or other drawings, specifications or other data are used for any purpose other than in connection with a definitely related government procurement operation, the U. S. Government thereby incurs no responsibility, nor any obligation whatsoever; and the fact that the Government may have formulated, furnished, or in any way supplied the said drawings, specifications, or other data is not to be regarded by implication or otherwise as in any manner licensing the holder or any other person or corporation, or conveying any rights or permission to manufacture, use or sell any patented invention that may in any way be related thereto.

402 337

63-3-2

402337

Columbia University in the City of New York

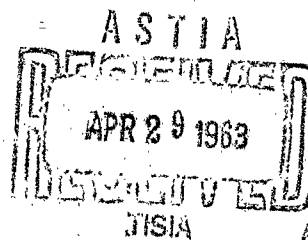
LAMONT GEOLOGICAL OBSERVATORY  
PALISADES, NEW YORK

MAGNETIC TOTAL  
INTENSITY MEASUREMENTS  
IN THE DRAKE PASSAGE

by  
George Peter

Technical Report No. 5  
CU-5-62 Nonr-Geology  
Contract Nonr 266(48)

October 1962



CATALOGED BY  
AS AD NO. \_\_\_\_\_

**Best  
Available  
Copy**

LAMONT GEOLOGICAL OBSERVATORY

(Columbia University)

Palisades, New York

MAGNETIC TOTAL INTENSITY MEASUREMENTS

IN THE DRAKE PASSAGE

by

George Peter

Contract Nonr  
266 (48)

Technical Report No. 5

CU-5-62-Nonr - Geology

October 1962

## CONTENTS

	Page
ILLUSTRATIONS	ii
INTRODUCTION	1
INSTRUMENTATION	2
MAGNETIC TIME VARIATIONS	4
MAGNETIC TOTAL INTENSITY PROFILES	6
MAGNETIC TOTAL INTENSITY CONTOUR MAP	10
GENERAL GEOLOGY OF TIERRA DEL FUEGO	11
MAGNETIC TOTAL INTENSITY ANOMALY MAP AND ITS INTERPRETATION	12
ACKNOWLEDGEMENTS	16
REFERENCES	17

## ILLUSTRATIONS

### FIGURE

- 1 Map of Drake Passage showing the location of the presented magnetic total intensity profiles.
- 2 Magnetic total intensity profiles  $B_1$   $B_2$
- 3 Magnetic total intensity profiles  $C_1$   $C_2$
- 4 Magnetic total intensity profile D with bottom topography
- 5 Magnetic total intensity profiles A, F, E
- 6 Magnetic total intensity profiles G, H
- 7 Magnetic total intensity profiles K, M, P, Q
- 8 Magnetic total intensity profiles I, J, L, O, N
- 9 Magnetic total intensity contour map
- 10 Geological map of southern Patagonia and Tierra del Fuego
- 11 Magnetic total intensity anomaly map.
- 12 Magnetic total intensity anomaly profiles with bottom topography near Tierra del Fuego
- 13 Calculated magnetic total intensity anomalies over cross section B of Figure 12.

## INTRODUCTION

From 1958 to 1962 the Lamont Geological Observatory obtained magnetic total intensity measurements over 5500 nautical miles of track between Tierra del Fuego, S. America, and Palmer Peninsula, Antarctica. Most of the measurements were made by the R/V VEMA of the L.G.O., and the A.F.T. YELCHO of the Chilean Navy Hydrographic Office. In the vicinity of the Tierra del Fuego additional measurements were made by the A.R.A. CAPITAN CANEPA and the A.R.A. GENERAL ZAPIOLA, both of the Argentine Navy Hydrographic Office.

The magnetic measurements are part of the geophysical program on the VEMA since 1952. The measurements on the YELCHO were made in 1961 and 1962 as part of the cooperative expedition program between the two organizations. On the CANEPA the measurements were obtained in 1958 with an instrument which was loaned to the Argentine Hydrographic Office, for the I.G.Y. and on the ZAPIOLA in 1962 these measurements were again part of a cooperative geophysical program.

In 1958-1959 the tracks of VEMA-14 and VEMA-15 cruises are near the Tierra del Fuego, and they reach further south only in the Scotia Sea. In 1960 the VEMA-16 cruise crossed part of the Drake Passage as the ship headed for Ushuaia from Wellington. In 1961 and 1962 The VEMA-17 and VEMA-18 cruises and the YELCHO-1 and YELCHO-2 cruises gave



several crossings over the Drake Passage, and additional coverage on both the Antarctic and the Tierra del Fuego shelves.

Figure 1 shows the map of the discussed area, and those parts of the tracks where the magnetic measurements are presented.

In the vicinity of Tierra del Fuego (area indicated on Figure 1) the tracklines are close to each other. In this report a magnetic total intensity map is shown from this area, and one of the anomalies is discussed in some detail. This anomaly is interpreted as due to a ridge, which extends from the continental shelf in the Cape Horn vicinity towards ESE about 100 miles.

#### INSTRUMENTATION

During V-14, V-15, a small portion of V-16, and during the CANEPA cruises a fluxgate magnetometer was used. This instrument is a modification of the ANASQ/3A airborne magnetometer, various versions of which have been widely used before the new absolute instruments. The Lamont model has been described by Heezen et.al. (1953).

This instrument is only mentioned for the sake of completeness, since all the reported measurements here were made with a proton precession magnetometer. The earlier fluxgate measurements are only used to show the trends on the

magnetic contour map where no absolute measurements are available.

During V-16, V-17, V-18, YELCHO-1, YELCHO-2 and ZAPIOLA-1 proton free-precession magnetometers were used. These instruments have been built and developed at Lamont, and the various versions have been described by Luskin and Hubbard (1959), Hirshman and Luskin (1960), and Heirtzler (1961). The present model is similar to other proton precession magnetometers in common use. Water is used for proton source, and to simplify operation, and gain more sensitivity the period of the precession frequency is measured, instead of the frequency itself. If the magnetic field changes, then the time for a given number of proton cycles changes also, and this time variation measured with  $10^{-5}$  sec accuracy is recorded on the original records. From the time, and from the selected precession cycles one can calculate the precession frequency. This frequency,  $f$ , is related to the magnetic field strength,  $F$ , by the equation

$$F = \frac{2\pi}{g'} f$$

where  $g'$  is the proton gyromagnetic ratio. ( $2.6713 \times 10^4$  radians/gauss second (Nelson 1960)).

For the different magnetic field strengths different numbers of proton precession cycles were selected to keep the full scale recorder range between 300 to 700 gammas.

When the instrument is set at 700 gamma full scale range the instrumental error is  $\pm .7$  gamma. Because of a slower electronic clock, the YELCHO-1 and the V-16 cruises had an instrumental error of  $\pm 7$  gamma. Instrument difficulties in the V-18 cruise caused the instrumental error to become  $\pm 15$  gamma on numerous occasions. Data with less instrument accuracy has been rejected. With the normal 300 to 700 gamma recorder range the other error sources, such as magnetic field of the ship and record reading and computational errors, are insignificant compared to the errors which came in by navigational uncertainty, and magnetic field variations. At the V-18 cruise, because of the low sensitivity in certain areas the record reading error is estimated to reach  $\pm 50$  gamma.

#### MAGNETIC TIME VARIATIONS

Since the magnetic data in this report represents several years of surveys, in order to compare the data one has to consider the long period (secular) magnetic variations first.

It was found at track crossings in the vicinity of Tierra del Fuego that the yearly change of the magnetic field is approximately -150 gamma, which is in close agreement with the value given on the U.S. Navy Hydrographic Office, Chart No. 1703, for the year 1955. It is difficult to check the yearly variations at track crossings further in the Drake

Passage because the weather there prohibits frequent astronomical fixes, and this causes navigational errors and, also, because the large number of magnetic anomalies along the track make the exact determination of the crossings difficult. Using the yearly magnetic change value from the above mentioned chart, however, gave good results, considering the other time variations and the already mentioned restrictions.

In this report the year is indicated on the profiles presented and in the comparison of them the secular variation has to be accounted for. Those magnetic profiles which were used in the preparation of the total intensity contour map were reduced to 1961 value since most of the coverage was obtained in that year.

There have been no corrections for the diurnal or the shorter period variations of the magnetic field. There are two reasons for neglecting the diurnal variation. The first reason is that for most areas in the southern hemisphere there is no time control data because of the sparsely spaced magnetic observatories. The second reason that in most magnetic mid-latitudes the diurnal variation is small, and its period is much longer than the period of the anomalies observed on a moving ship. In any case additional reduction work for removing time variations would only be profitable for surveys with closely spaced control lines.

It is expected that the average day diurnal variation (mean all days) is the same in our survey area as it

is at a similar northern magnetic latitude, which is a peak to peak value of 50 gamma. (Vestine et.al. 1947)

Shorter period variations ( $S_D$ ,  $D_{st}$ ) might also have effected the data. The separation of the effect of these from the anomalies, even with observatory data, would be possible only in special cases because their period is equal to that of the anomalies. The most expedient procedure was to check the three hour K indices and omit the data on internationally disturbed days, or at such areas where the higher K indices represent comparable or much higher gamma changes than the expected anomalies.

During the time of the survey, near Tierra del Fuego, the K indices did not indicate that such omissions were necessary. The other profiles are presented as they were observed regardless of the K index value.

#### MAGNETIC TOTAL INTENSITY PROFILES

Figure 2 to Figure 8 shows the magnetic total intensity profiles. Each profile shows the magnetic total intensity values in gammas ( $10^{-5}$  gauss) as a function of distance in nautical miles. The local times (time zone +4) are also shown at important course changes, some navigational fixes and at ship starting points. The ship stops on the profiles are marked and the corresponding times can be found on Figure 1 together with the other time marks of the profiles.

Table 1 gives the date interval for each profile and the cruise number. The profiles are made with the earlier times on the left side.

Table I  
Cruises and Dates of Profiles

Profile	Date From	Date To	Cruise
A	Feb. 26, 62	Feb. 27, 62	V-18
B <sub>1</sub>	Feb. 25, 62	Feb. 26, 62	Y-2
B <sub>2</sub>	Feb. 26, 62	Feb. 27, 62	Y-2
C <sub>1</sub>	April 14, 61	April 15, 61	V-17
C <sub>2</sub>	April 15, 61	April 17, 61	V-17
D	March 7, 62	March 8, 62	Y-2
E	April 27, 61	April 27, 61	V-17
F	May 6, 60	May 7, 60	V-16
G	Feb. 27, 62	March 2, 62	Y-2
H	Feb. 27, 62	March 3, 62	V-18
I	April 18, 61	April 18, 61	V-17
J	April 18, 61	April 20, 61	V-17
K	April 20, 61	April 21, 61	V-17
L	March 5, 62	March 6, 62	V-18
M	March 5, 62	March 6, 62	Y-2
N	March 4, 62	March 5, 62	V-18
O	March 3, 62	March 4, 62	V-18
P	March 7, 62	March 8, 62	Y-2
Q	April 21, 62	April 22, 62	V-17

The magnetic profiles A through Q are not all of the magnetic data that has been collected in the past years. In an area near Tierra del Fuego the track distances were close enough to prepare a magnetic total intensity map, and the data is presented in that form for that area. Additional short profiles are available on the Tierra del Fuego shelf between the Magellan Strait and Cape Horn, and on the V-16 and V-18 Drake Passage crossings. These profiles will be presented at a later date.

Profiles A, B<sub>1</sub>, B<sub>2</sub>, C<sub>1</sub>, C<sub>2</sub>, E and D are nearly perpendicular to the arc of Tierra del Fuego and the Palmer Peninsula. B<sub>1</sub>, B<sub>2</sub> and F are in the direction of the maximum magnetic field change, therefore, these profiles were used to determine the regional gradient. The value of the regional magnetic field change is approximately 14 gamma per nautical miles. Profiles G and H are nearly in the direction of equal intensity lines, therefore, only a very small regional change can be seen on them.

Profile D is a complete crossing of the Drake Passage and it is shown together with the bottom topography, (uncorrected soundings) in order to demonstrate that the magnetic anomalies are caused by subbottom structural changes rather than by bottom topographic relief. The topographic trends, however, frequently reflect the structural trends. Comparing profiles G and H, the trend of the magnetic

anomalies lie in a SW-NE direction, which is, according to Heezen's physiographic diagram (Heezen and Tharp 1961), also the direction of the topographic trend. Profile J, further to the north, shows E-W magnetic trend, which is the direction of the topographic trend there too.

Profiles M, P and the end of G are crossings of the Palmer continental shelf. The similarity between P and G is striking. The seven hundred gamma anomaly at the end of Profile G can be found at the beginning of Profile P (West of V. Hugo Island) and Profile M starts very close to the north of it. Profiles K and L stop before reaching the anomaly. Profile Q, which is at the extension of K, however, shows the same anomaly with large disturbances on it which indicate the presence of basic igneous rocks near the observation line. Additional measurements are needed to establish this trend, but the present data seems to indicate that the same volcanic rocks which formed the South Shetland Islands are extending SW buried under the sediments and forming V. Hugo Island, 150 nautical miles away. Profile M indicates that the anomaly causing structure is close to the ocean bottom, while under Profiles G and P it must be at a deeper level.

Profiles I, J, K, L, N and O are too far apart, and their direction is too random to allow comparison.



MAGNETIC TOTAL INTENSITY CONTOUR MAP

Figure 9 shows the magnetic total intensity contour map and the track lines used in its construction. The track indicated by "a" was accepted as basic and the other tracks were adjusted to its position. Track "b" was moved 7 miles S.W., track "c" 3 miles W., and two short fluxgate magnetometer tracks on the west side of the map were moved 4 miles S.E. These adjustments are justified since the cloud conditions, strong winds and currents make navigation uncertain in this area. The easterly tracks were only used to extend the trend of the contour lines, therefore, their position has not been adjusted.

The magnetic measurements were reduced to 1961 total field values because most of the proton precession magnetometer data was obtained in that year. Time variations are not corrected except on track "a" where the values on the northern part were exceptionally high compared to the other measurements on the crossing tracks.

Slanted broken lines on the west indicate an area where the contour map represents a smoothened total intensity picture. Here this area is characterized by short period large magnetic anomalies, which could not be contoured with the present survey line interval. Additional survey lines are needed to check for a possible extension of the local anomalies on the E-SE tracks of the map.

GENERAL GEOLOGY OF TIERRA DEL FUEGO

In Figure 10 a geological map of southern Patagonia and Tierra del Fuego is presented. (G.S.A. 1950). The area can be divided into two sections: the first is the Patagonian Cordillera, the second is Extra-Andean Patagonia, which extends from the Cordillera to the Atlantic coast.

Extra-Andean Patagonia consists of tablelands. It is covered mostly by Quaternary and Tertiary continental sediments. The Cretaceous is represented by marine sediments, the Jurassic by the "Serie Porfirica" (mostly marine sediments), which, according to drilling and seismic information, are considerably thinner toward the east. The interbedded tuffs and lavas (acidic) are the consequence of Jurassic, Oligocene and Pliocene orogenic movements.

The Patagonian Cordillera can be divided into three parts. On the north-northeast, Cretaceous marine sediments are on the surface, and together with the "Serie Porfirica" these form a section several thousand meters thick. Toward the south the Pre-Cretaceous metamorphic rocks form a narrow belt, and south of that are the intrusives of the Andean Batholith, which was formed during the Middle Cretaceous orogenic movements. This whole south-western coastal area was subjected to block faulting during the Oligocene and Pliocene, with renewed volcanic activity in the Pliocene.

The igneous rocks of this region represent a broad

spectrum from acidic to basic. During a recent reconnaissance geological survey by the Empresa Nacional del Petroleo Magallanes, basic rocks were found on Deceit Island, and Lennox Island, and form the Pico and the Dientes de Navarino mountains on Navarino Island. Diorite was found on Hermite Island and on Snipe Island. Magnetic surveys indicate the presence of basic rocks on the Wollaston Islands, on Cape Horn, and in the vicinity of Murray Channel, Clockburn Channel and Cook Bay. On the basis of presently available data these basic rocks appear to occur in a 10 to 20 miles wide belt in the south-west Cordillera, and their presence was indicated by magnetic measurements over a distance of 800 miles towards the north.

#### MAGNETIC TOTAL INTENSITY ANOMALY MAP, AND ITS INTERPRETATION

The magnetic total intensity anomaly map (Figure 11) was obtained by placing a regional grid over the total intensity map and subtracting the regional field value from the total field value at their crossings. The regional grid was prepared on the basis of the total intensity map.

On the anomaly map several areas can be distinguished by their magnetic trends and character. The magnetic field is relatively uniform in an area N.W. from Long.  $64^{\circ}30'W$ , Lat.  $56^{\circ}S$  until Tierra del Fuego, in the neighborhood of Long.  $65^{\circ}W$ , Lat.  $57^{\circ}S$ , and along Long.  $62^{\circ}30'W$  from Lat.  $56^{\circ}S$  north.

Centered approximately along  $64^{\circ}\text{W}$  longitude, several anomalies exhibit north-south trend. The last one mapped at Lat.  $57^{\circ}\text{S}$  seems to have extension toward the east. At  $56^{\circ}20'\text{S}$  there is an approximately hundred miles long anomaly which extends between Cape Horn and the previously mentioned north-south trending anomalies. Indicated by slanted broken lines, in the Cape Horn vicinity and south of it, there is an area which exhibits several short period anomalies.

The magnetically undisturbed areas usually represent thick sediments, or deep uniform magnetic basement, or the combination of these. The uniform magnetic field near Tierra del Fuego is probably due to the thick Tertiary marine sediments, while the other two magnetically undisturbed areas fall into the second category since the bottom depth alone is 2000 fathoms there.

The north-south trending anomaly group coincides with a submarine mountain range (Heezen, Tharp, 1961), which terminates at approximately Lat.  $57^{\circ}\text{S}$  and turns east. The relatively broad anomalies are indicating that the mountains consist of igneous rocks, the narrow peaks indicate basic intrusions or dikes in places from Lat.  $56^{\circ}\text{S}$  south.

The east-west trending anomaly is interpreted as the extension of the Andean batholith, which appears to terminate at, or offset by, the north-south mountain range. Figure 12<sub>A</sub> shows two crossings of this anomaly and the submarine topography on the continental shelf, Figure 12<sub>B</sub> shows three

crossings in deep water. The track  $S_1$  crosses the anomaly south-west of Cape Horn,  $S_2$  at the edge of the continental shelf, A and B in deep water. The corresponding ridge clearly can be seen on tracks  $S_2$ , A and B. Track C crosses the ridge as it enters the area of the north-south mountain range.

At crossing B the magnetic anomaly has been calculated over a pair of two dimensional bodies (Girdler and Peter 1960, Heirtzler, et.al. 1962), which had a simple geometrical cross section (Figure 13). It was assumed that the magnetization is due to the earth's present induced field; total field strength  $F = 37200$  gammas, inclination  $I = -51^\circ$ ; and that the declination is perpendicular to the strike of the body. Susceptibilities of .009 cgs. and .006 cgs. were required to match the observed anomaly, which values represent magnetizations of .0033 cgs. and .0022 cgs. respectively.

On Figure 13 a solid line represents the observed anomaly, dotted lines represent the calculated anomalies over the two models, and a broken line shows the combined calculated anomaly.

Smaller susceptibility value is sufficient for model "a" (indicated by slanted lines), if we assume that the direction of the magnetization of model "b" is different from the direction of the present earth field. A  $10^\circ$  steeper direction of magnetization ( $-60^\circ$ ) at this model would increase

the maximum and would reduce the minimum of the calculated anomaly curve, which in turn when combined with the calculated anomaly curve "a", would give a better match with the observed curve, and would allow lower susceptibility for model "a".

Model "a" can be interpreted as part of the Andean intrusions where basic igneous rocks are dominant, or could represent an area where contemporary or later volcanic activity produced basic igneous intrusions. Model "b" is the less basic part of this system, which together with the basic igneous facies forms most of the islands south of Tierra del Fuego. Since diorite represents the less basic rocks of the batholith in this vicinity, the assumption of remanent magnetization with equal strength to the induced magnetization is reasonable, because this would allow a susceptibility of .0029 cgs., which is much more fit to the diorite than the value that was necessary for the calculation. (Nagata 1956, Books 1962).

The models represent a simple approximation of a very complex geology, which cannot be studied directly, therefore, instead of using additional arbitrary assumptions the present fit of the observed and calculated anomalies was accepted.

The anomalies in the Cape Horn vicinity and toward the south indicate the subbottom topography relief, and the structural change in these basic rocks, which in that area

- are much closer to the observation line (sea surface) allowing greater resolving for the instrument.

#### ACKNOWLEDGEMENTS

This work was supported by the U.S. Navy under Contract Nonr 266(48) with the Office of Naval Research, and the National Science Foundation, Grant 4151. Reproduction of this document in whole, or in part, is permitted for any purpose of the United States Government.

Lamont personnel assisting in obtaining the magnetic data were: P. Chelminski, I. Gereben, W. Pitman, L. Burkle; the data reduction and drafting work was done by: C. Peppin, J. Maxon, D. Brubaker and D. Wolfe.

Special appreciation goes to Capt. G. Barros of the Chilean Navy Hydrographic Office and Capt. L. Capurro of the Argentine Navy Hydrographic Office for making the joint geophysical surveys possible; and for the Captains of the cooperating vessels, Cmdr. G. Alfaro and Cmdr. R. MacIntyre of the Chilean Navy and Lt. Granelli of the Argentine Navy, and their crews for their invaluable assistance in various parts of these surveys.

The information on the geology of Tierra del Fuego was given by Mr. Eduardo Gonzales of the Empresa Nacional del Patroleo Magallanes, and it is greatly appreciated.

## REFERENCES

- Books, K.G., 1962; Remanent Magnetism as a Contributor to some Aeromagnetic Anomalies: Geophysics Vol. XXVII, No. 3, pp. 350-375.
- Girdler, R.W., and G. Peter, 1960; The Importance of Natural Remanent Magnetization: Geophys. Prospecting, Vol. VII, No. 3, pp. 474-483.
- Heezen, B.C., M. Ewing, E.T. Miller, 1953; Trans-Atlantic Profile of Total Magnetic Intensity and Topography, Dakar to Barbados: Deep-Sea Res., Vol. I, pp. 25-33.
- Heezen, B.C., M. Tharp, 1961; Physiographic Diagram of the South Atlantic Ocean: Geological Society of America Publication.
- Heirtzler, J.R., G. Peter, M. Talwani and E.G. Zurflueh, 1962; Magnetic Anomalies caused by Two-Dimensional Structure Their Computation by Digital Computers and Their Interpretation: C.U. Technical Report in preparation.
- Heirtzler, J.R., 1961; Vema Cruise No. 16 Geomagnetic Measurements: C.U. Technical Report No. 2.
- Hirshman, J., and B. Luskin, 1960; A Two-Conductor Proton Precession Magnetometer for Marine Use: Unpublished Report.
- Hubbard, A.C., and B. Luskin, 1959; Sounding and Magnetometer Equipment for a Drifting Ice Station: C.U. Technical Report, CU-52-59.
- Nagata, T., 1956; Rock Magnetism: Maruzen, Tokyo.



Nelson, J.H.; Journal Geoph. Res., Vol. 65, No. 1.

(Nov. 1960) p. 3826.

Stose, G.W., 1950; Geologic Map of South America: Geological Society of America Publication.

Vestine, E.H., L. Lange, L. Laporte, and W.E. Scott, 1947;  
The Geomagnetic Field, its Description and Analysis:  
Carnegie Institution of Washington, Publ. No. 580.

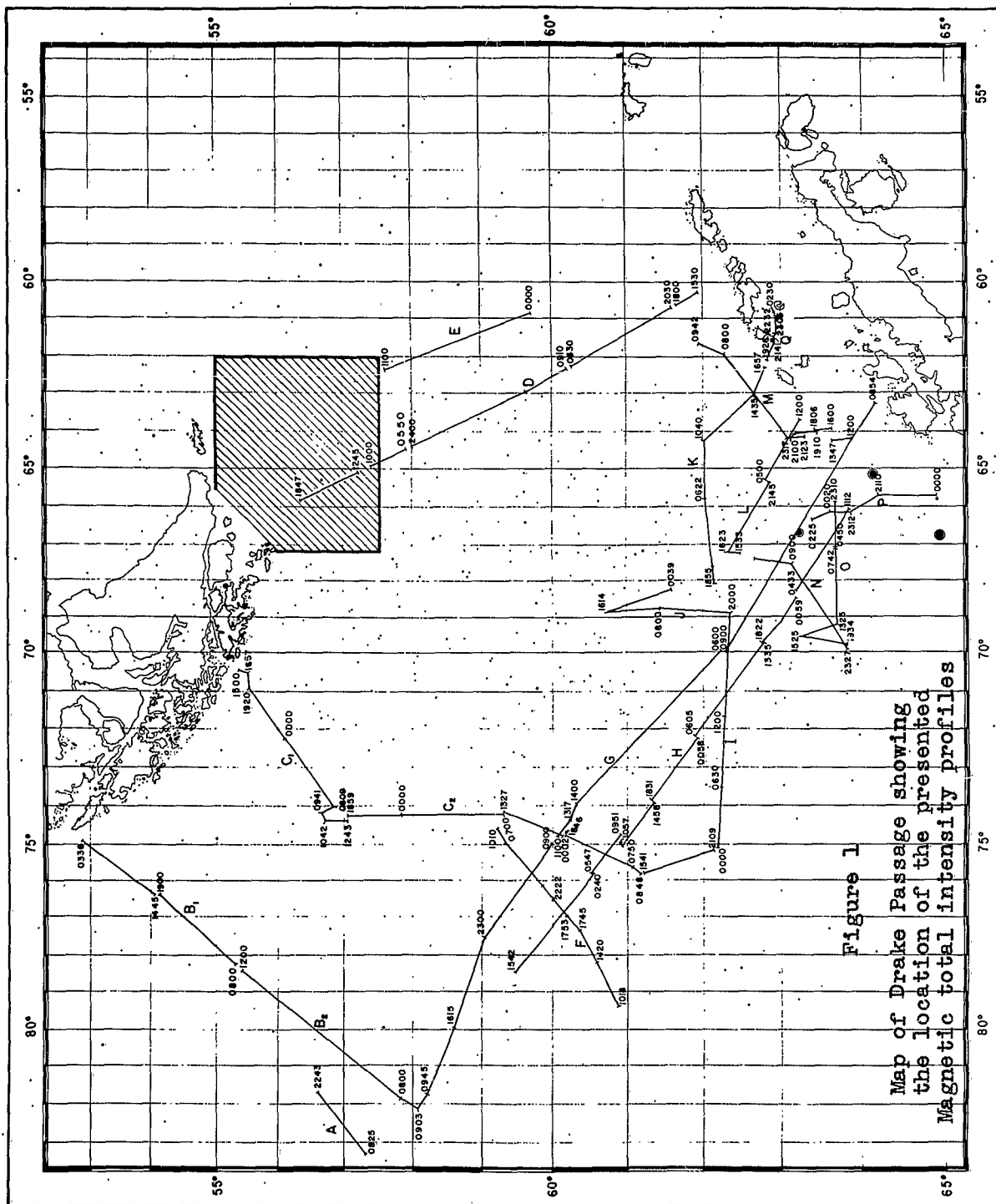


Figure 1  
Map of Drake Passage showing  
the location of the presented  
Magnetic total intensity profiles

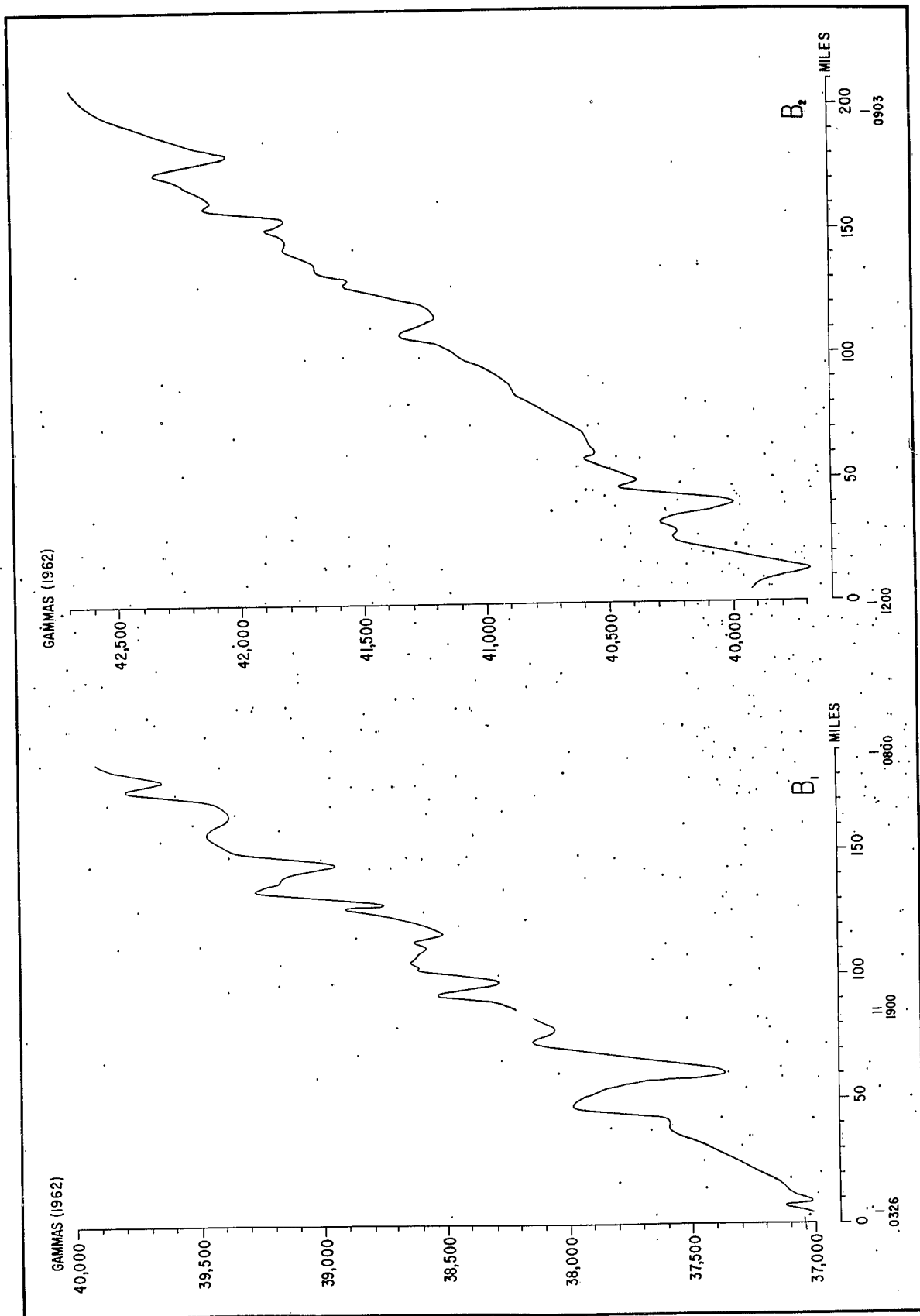


Figure 2: Magnetic total intensity profiles B<sub>1</sub> B<sub>2</sub>

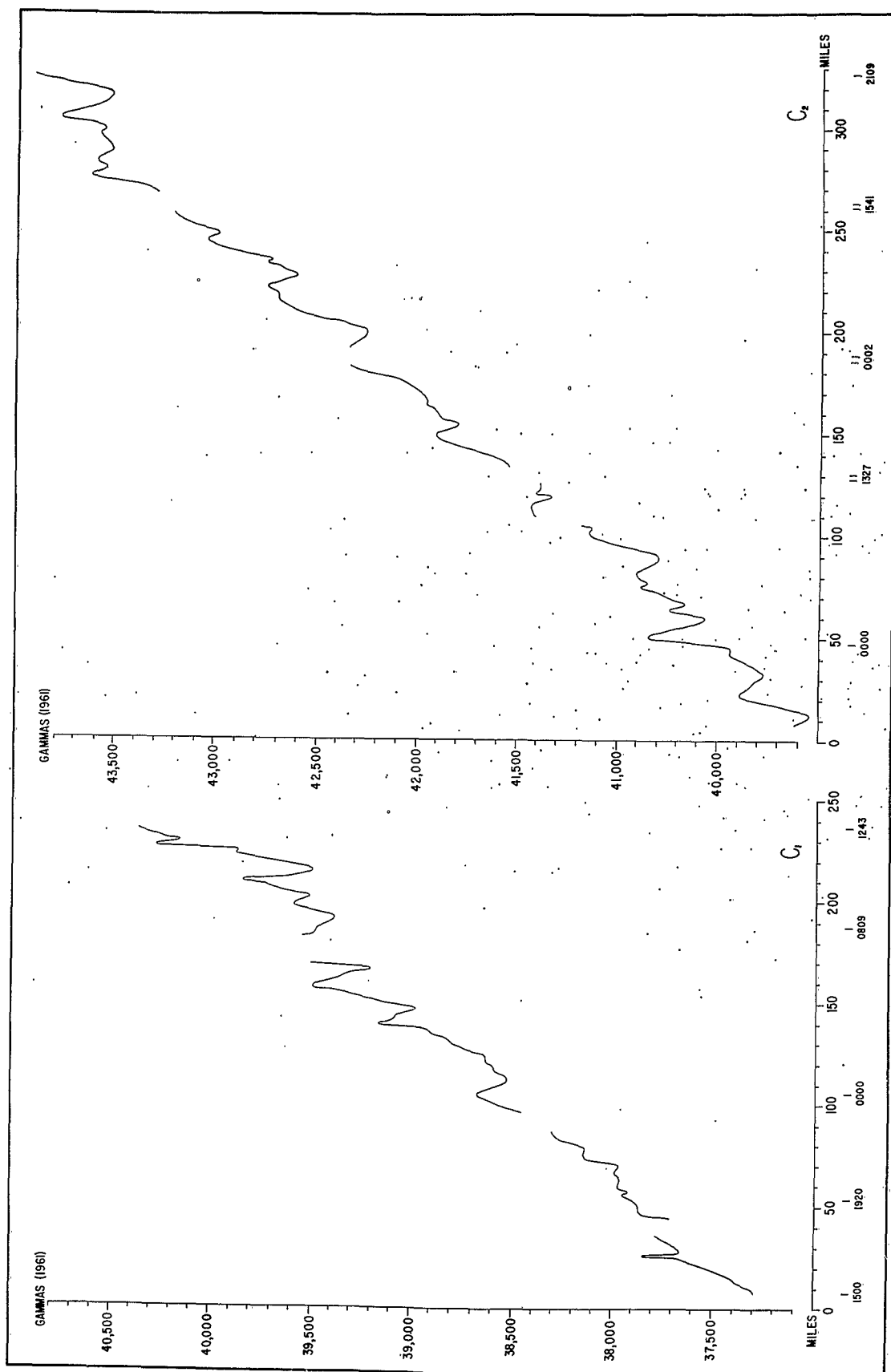
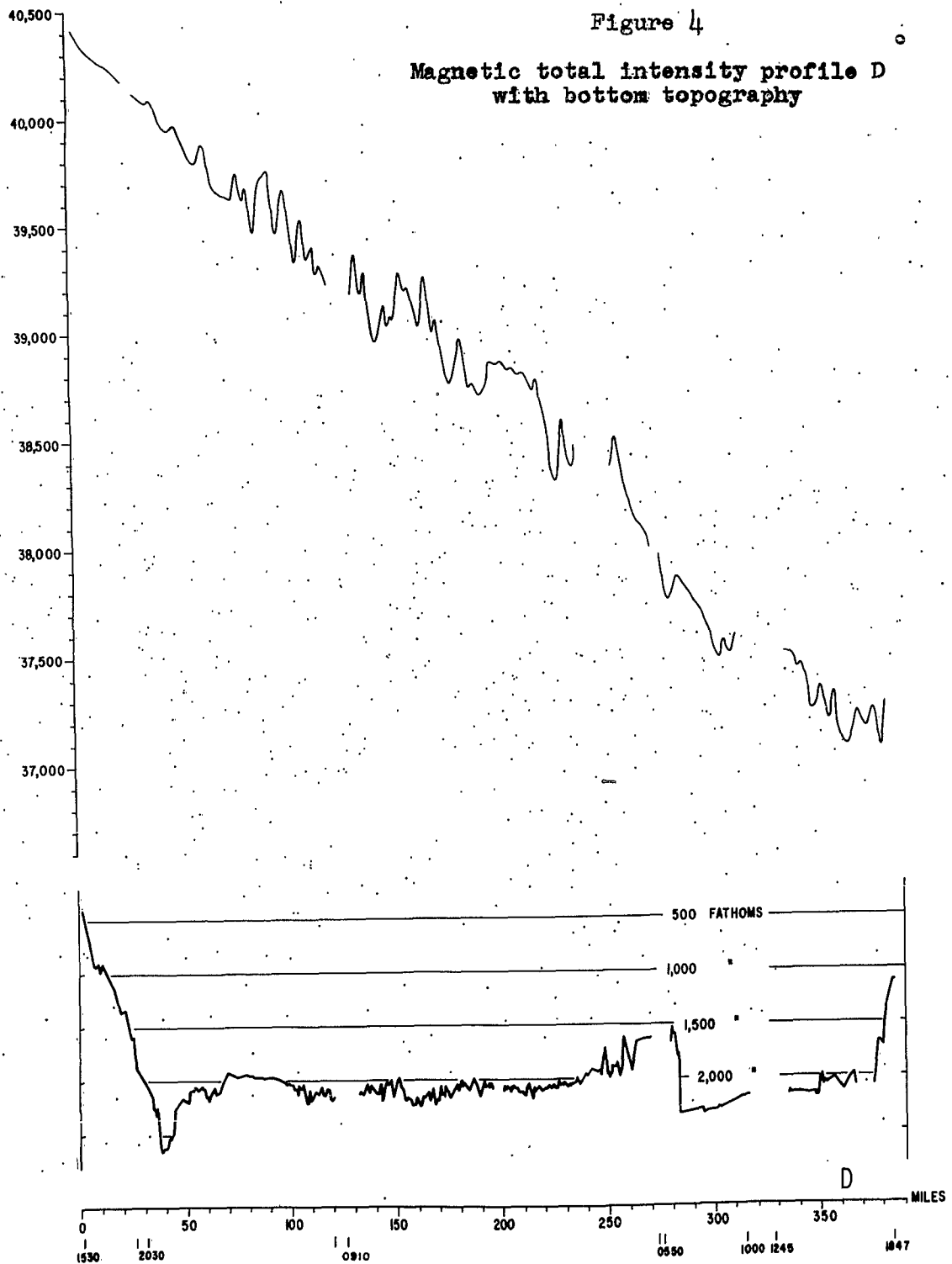


Figure 3: Magnetic total intensity profiles C<sub>1</sub> C<sub>2</sub>

Figure 4

Magnetic total intensity profile D  
with bottom topography



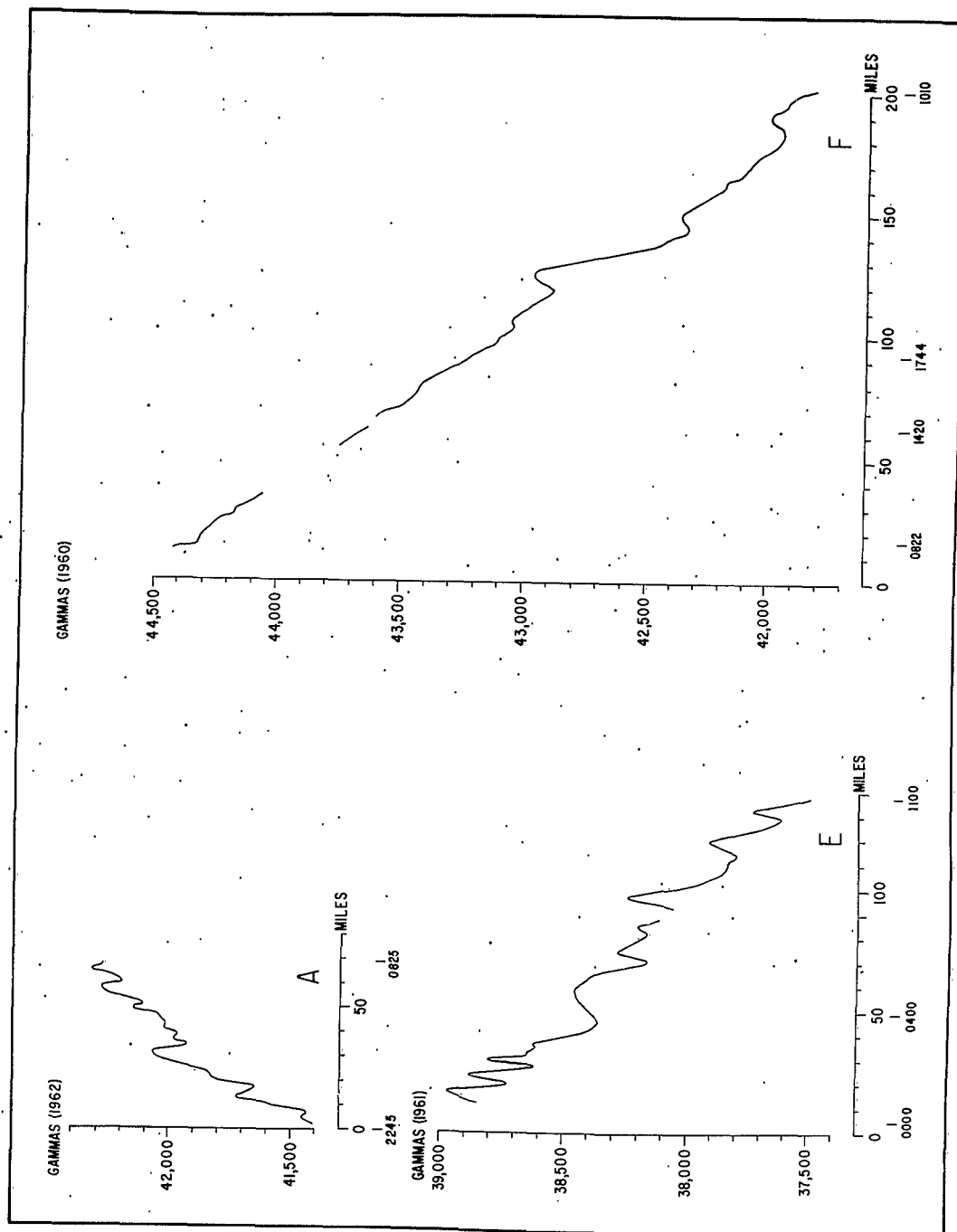


Figure 5: Magnetic total intensity profiles A, F, E

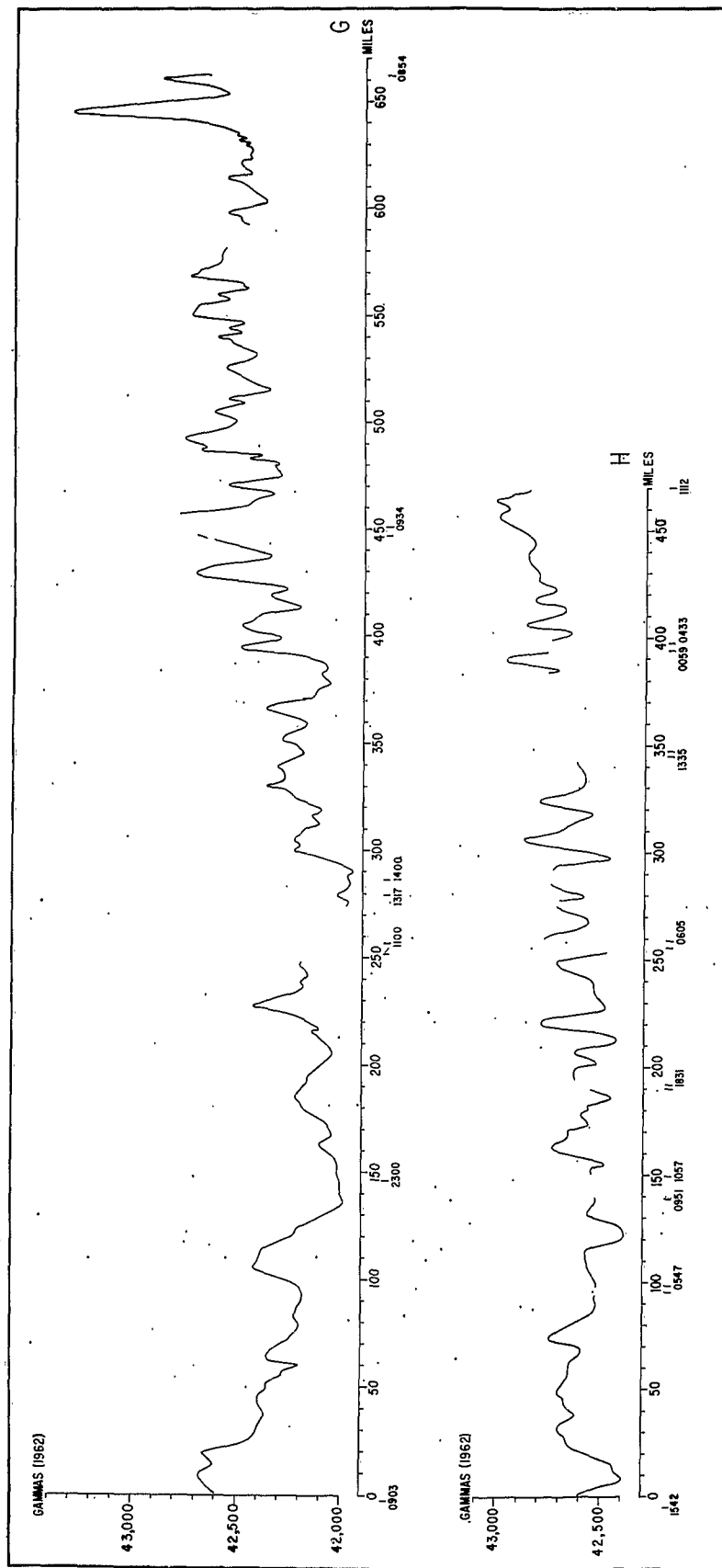


Figure 6: Magnetic total intensity profiles G, H

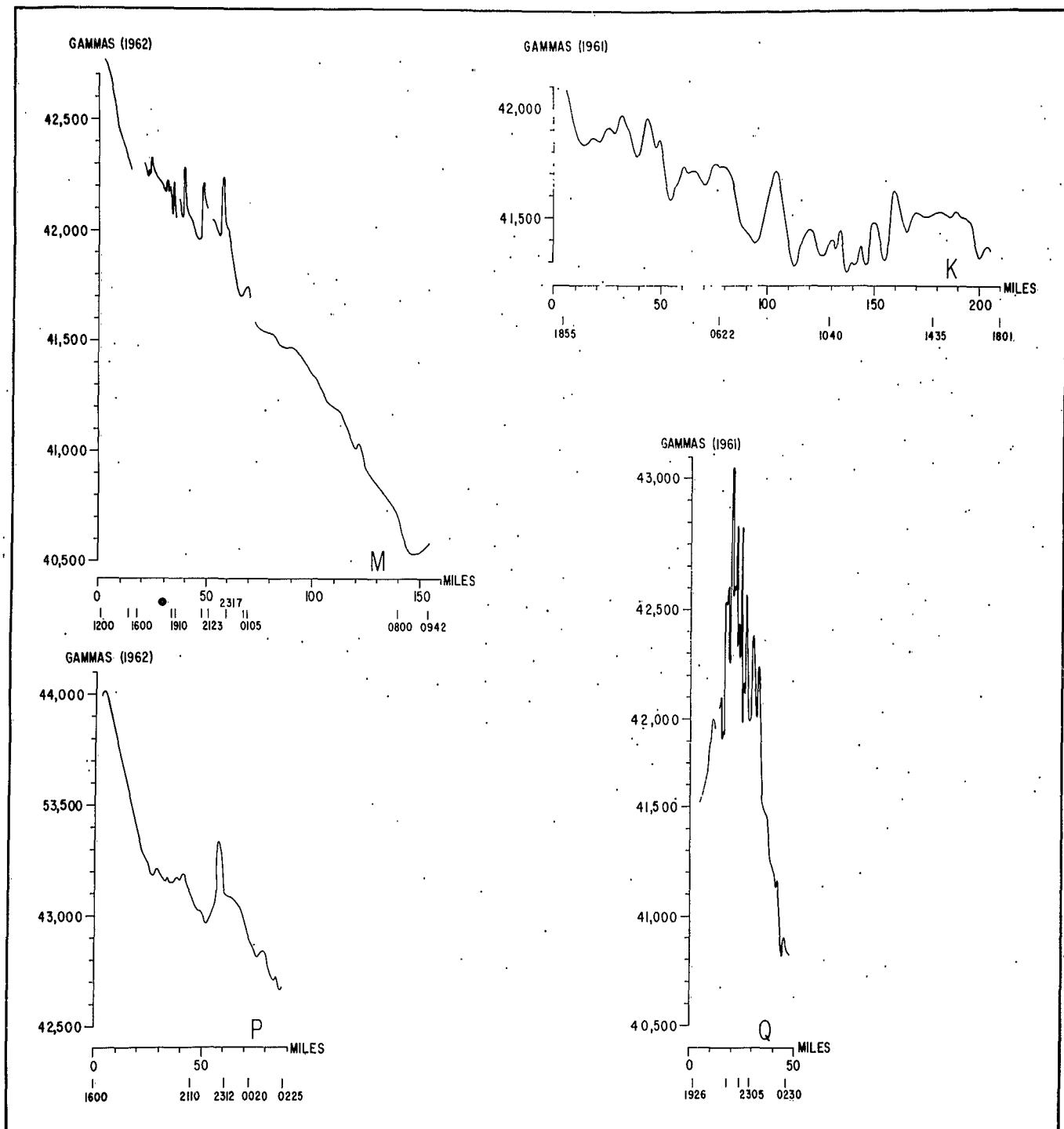


Figure 7: Magnetic total intensity profiles K, M, P, Q



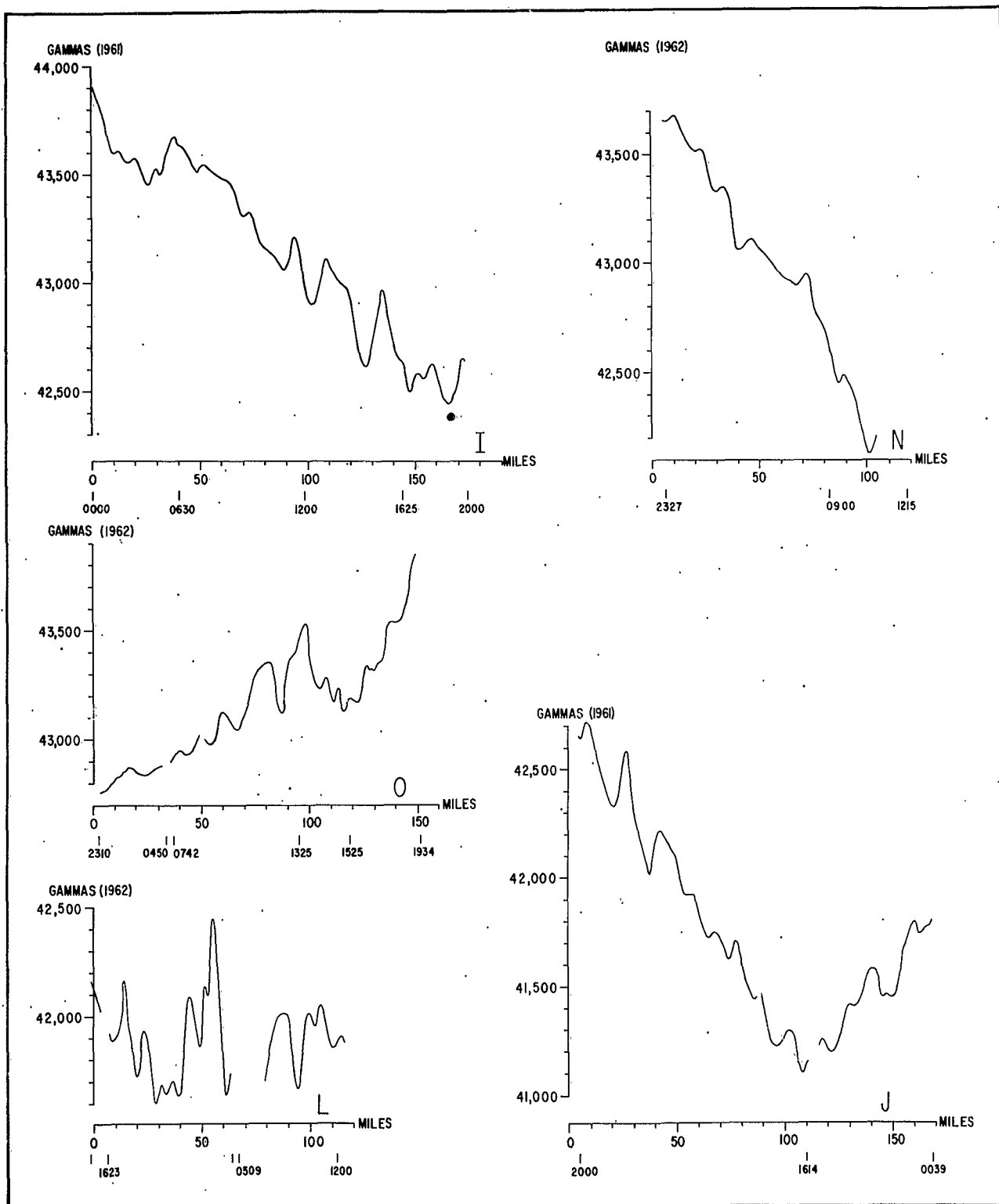
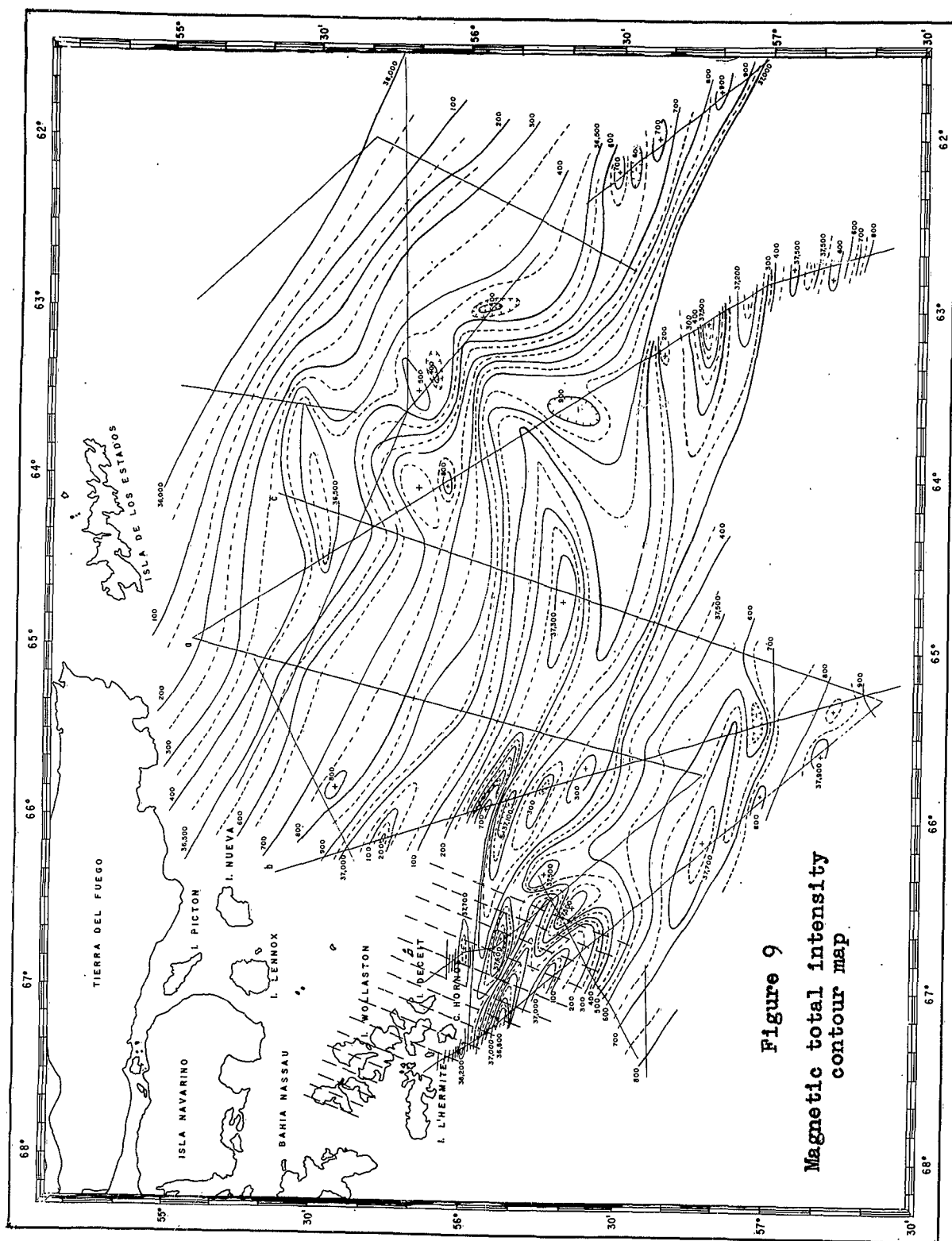


Figure 8: Magnetic total intensity profiles I, J, L, O, N



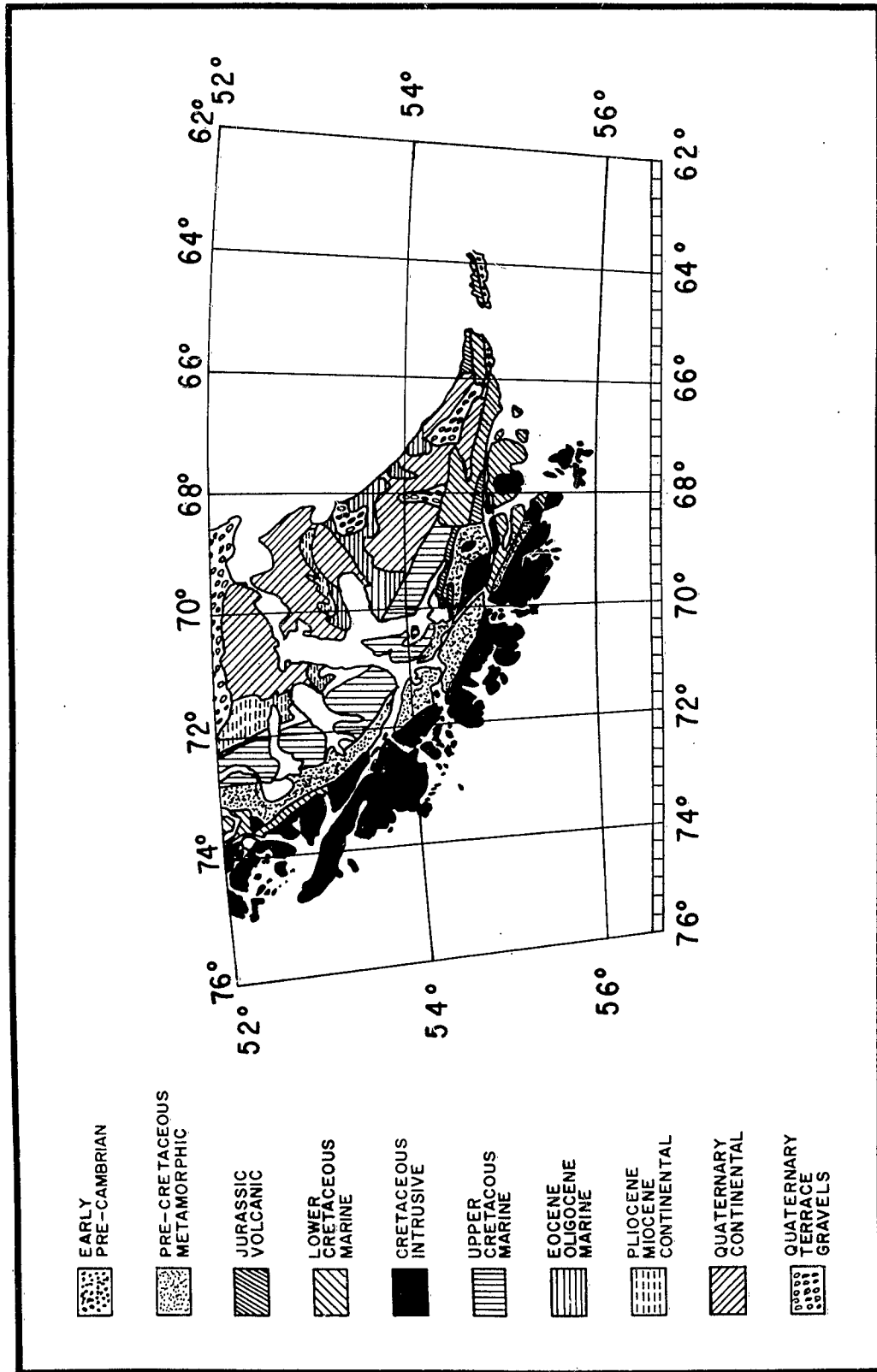


Figure 10: Geological map of southern Patagonia and Tierra del Fuego

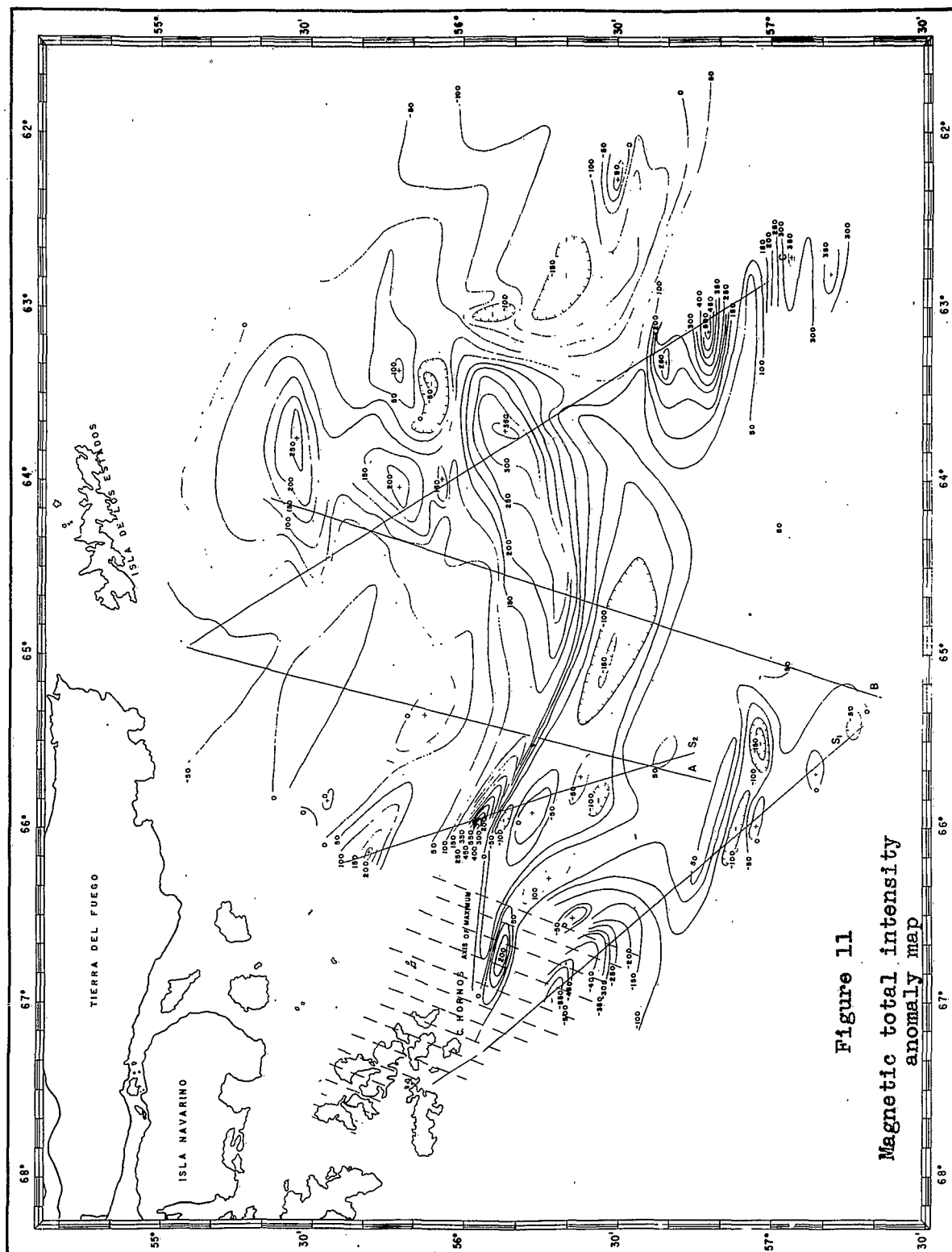


Figure 11  
Magnetic total intensity  
anomaly map

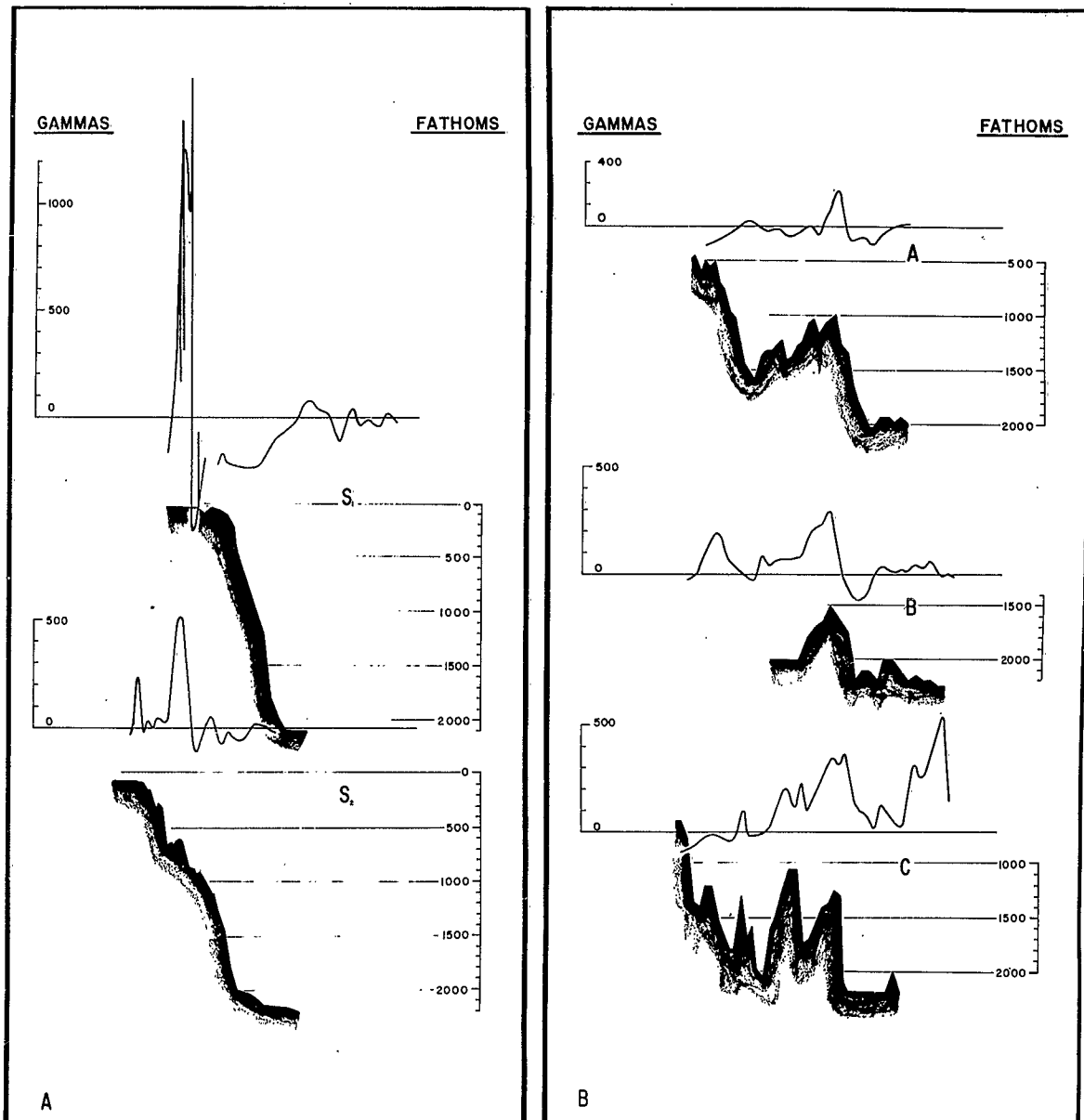


Figure 12

Magnetic total intensity anomaly profiles  
with bottom topography near Tierra del Fuego

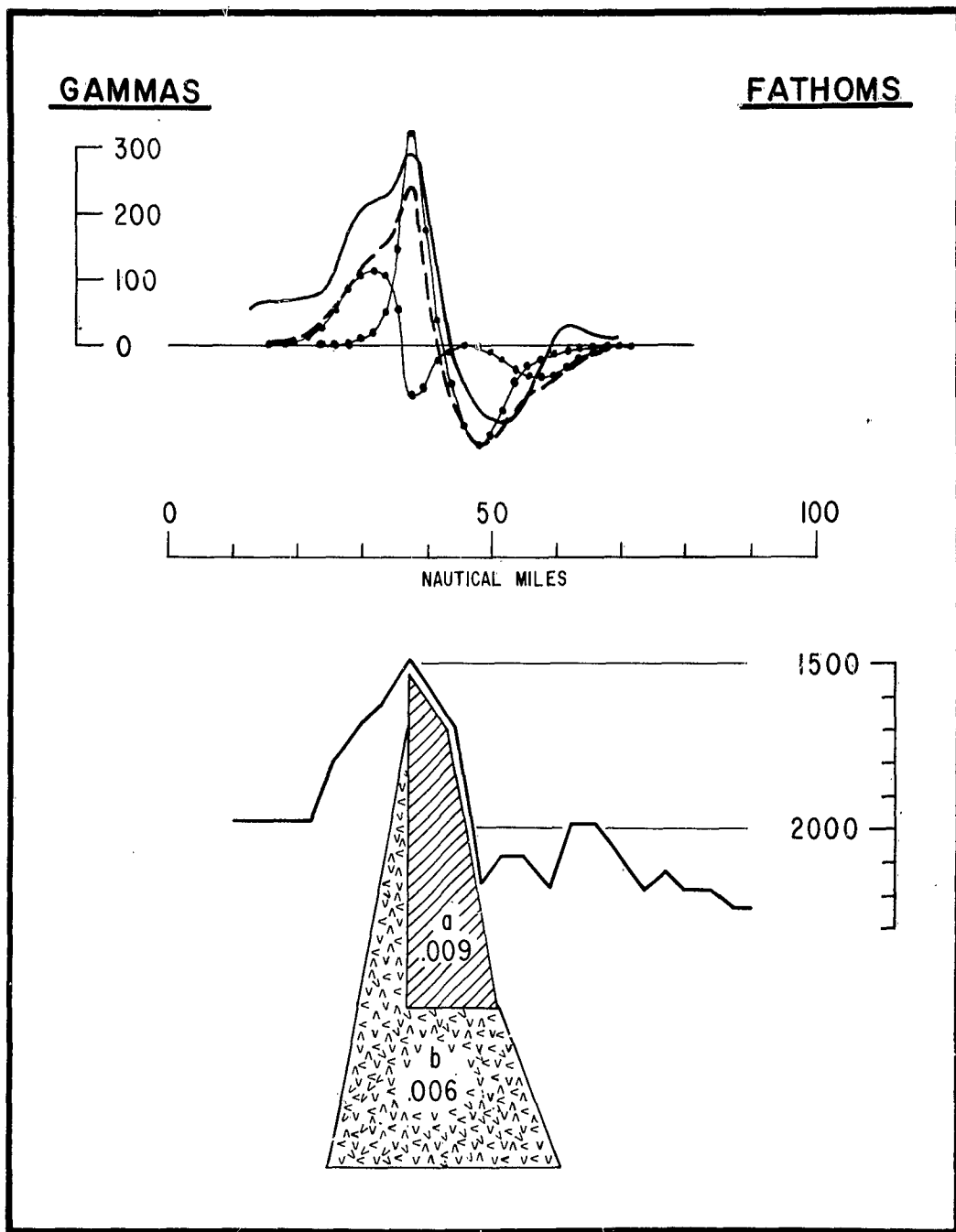


Figure 13

Calculated magnetic total intensity anomalies  
over cross section B of Figure 12